Clim Dyn
DOI 10.1007/s00382-016-3010-1

Tree-ring reconstructed May–June precipitation in the Caucasus since 1752 CE

Dario Martin-Benito[1,2] · Caroline C. Ummenhofer[3] · Nesibe Köse[4] · Hüseyin Tuncay Güner[4] · Neil Pederson[1,5]

Received: 16 July 2015 / Accepted: 26 January 2016

Abstract The Caucasus region experiences recurrent droughts that affect natural vegetation and the agriculture-based economies of several countries. Because meteorological records are in general scarce and of short timespan, little is known about the magnitude and frequency of past climate variability. Despite the recent increase of climate reconstructions for parts of Eurasia, no study has focused on past hydroclimate variability in the Caucasus. Here, we use a multispecies network of tree-ring width chronologies from the Lesser Caucasus to develop the first precipitation reconstruction for the region back to 1752 CE. Despite the high annual precipitation in the region, our reconstruction accounted for 51.2 % of the variability in May–June precipitation from 1930 to 2001. In comparison with reconstructions in the eastern Mediterranean, our new reconstruction revealed important and distinct drought periods and pluvials. Previous winter North Atlantic Oscillation (NAO), and spring East Atlantic/Western Russia (EA/WR) and North Sea Caspian patterns are likely key drivers of May–June precipitation in the Caucasus and Anatolia. NAO appeared to negatively affect rainfall low-frequency variability while effects of EA/WR were more apparent at the interannual timescales. We also show a potential positive effect of Black Sea surface temperatures on May–June precipitation. In the Caucasus, May–June represents the period of major water supply in semi-arid areas and the period with the highest potential of water scarcity in mesic areas. It is also a period of potential catastrophic flood events. Thus, changes to the precipitation regime during this season will be critical to both human and natural systems of the Caucasus region.

Keywords Anatolia · Black Sea · Dendrochronology · Drought · EA/WR · NCP · NAO · Precipitation

1 Introduction

Climate change is expected to have significant impacts in mid-latitude Europe and the Mediterranean basin through a decrease in summer precipitation (Giorgi and Lionello 2008). Over recent decades, however, the Caucasus region and the southeastern coast of the Black Sea have experienced different trends in precipitation than the eastern Mediterranean coast of Turkey (Levant) and the Fertile Crescent (Trigo et al. 2010). While the mountains of northeastern Turkey have experienced increasing cold season (November–April) precipitation, the eastern Mediterranean has been increasingly dry (Hoerling et al. 2012). Differences between the Mediterranean and eastern parts of the Anatolian peninsula and the Caucasus are expected to grow: in areas under stronger influence of the Black Sea

Electronic supplementary material The online version of this article (doi:10.1007/s00382-016-3010-1) contains supplementary material, which is available to authorized users.

✉ Dario Martin-Benito
dario.martin@usys.ethz.ch

1 Tree Ring Laboratory of Lamont-Doherty Earth Observatory, Columbia University, 61 Rt 9W, Palisades, NY 10976, USA

2 Present Address: Forest Ecology, Institute of Terrestrial Ecosystems, Department of Environmental Systems Science, ETH Zurich, Universitätstrasse 22, 8092 Zurich, Switzerland

3 Department of Physical Oceanography, Woods Hole Oceanographic Institution, Woods Hole, MA, USA

4 Forest Botany Department, Faculty of Forestry, Istanbul University, 34473 Bahçeköy, Istanbul, Turkey

5 Present Address: Harvard Forest, Harvard University, 324 North Main Street, 40, Petersham, MA 01366, USA

Published online: 08 February 2016

projections are for wetter conditions (Evans 2009), whereas precipitation is likely to decrease in the regions bordering the Mediterranean, and further inland to the Caspian Sea (Chenoweth et al. 2011). To date, increased drying in the Fertile Crescent has had devastating socio-economical effects, causing widespread crop failure in a region greatly dependent on rain-fed agriculture (Kelley et al. 2015).

The Caucasus region is infused with complex climatic patterns with steep precipitation and temperature gradients due to its location on the temperate-subtropical zone boundary, between the Black Sea and the Caspian Sea, and its complex topography (from sea level to >4000 m asl). The Colchic lowlands experience subtropical climate while the surrounding mountains receive enormous amounts of precipitation because of lake-effect and orographic forcing. The mild climate of the lowlands between the Greater and the lesser Caucasus has allowed for vast areas of land being dedicated to agriculture for millennia. The area has been home to ancient agricultural civilizations which have had great impact on its natural vegetation (Connor et al. 2007). The warm and moist climate in the area allows for the cultivation of some subtropical crops, such as *Citrus* sp. and tea (*Camelia sinensis*). Despite the large amounts of precipitation, the Caucasus has some of the highest variance in summer precipitation in northern Eurasia (Schubert et al. 2014). The north and central Caucasus have been historically major grain-producing regions where spring and early summer precipitation is critical for spring-grain maturation (Pavlova et al. 2014). For example, a strong drought is thought to have triggered a historical famine in 1931–1933 in the north Caucasus, although causes for the famine are still under debate (Tauger 2001). Despite the projected increase in precipitation for the wetter areas in the Caucasus, rising pressure on water resources is likely due to higher water demand to supply the growing population, agricultural production, and hydropower needs combined with reduced water availability in the surrounding semi-arid areas (Chenoweth et al. 2011). These pressures on water supply could become even greater if warming overwhelms increasing precipitation as some models forecast for the region (Cook et al. 2014).

Climate over the eastern Black Sea and the Caucasus is subject to complex atmospheric patterns. Year-round westerly circulation brings moist air over the Caucasus (Stanev and Rachev 1999), but these dynamics are affected by two anticyclones, one centered in western Russia during the winter and spring and a second one over Scandinavia and Western Europe during the spring (Golubev et al. 1993). Two main atmospheric teleconnections have been suggested to affect the rainfall patterns in the region. During winter, the North Atlantic Oscillation (NAO) affects precipitation in the Mediterranean, the Middle East, and central Anatolia (Cullen and deMenocal 2000; Türkeş and Erlat 2003). The distance between the Caucasus and the two main pressure centers of the NAO index may cause the influence of this winter teleconnection to be stronger at a certain time lag, in such a way that winter NAO may affect the following spring (Herceg-Bulić and Kucharski 2014). NAO also has a lagged influence (2–3.5 years) on Black Sea surface temperatures (Buongiorno Nardelli et al. 2010). In addition, winter climate in eastern Turkey, the Caucasus and central-western Eurasia is also affected by the East Atlantic/Western Russia pattern (EA/WR) (Oguz et al. 2006; Xoplaki et al. 2004) or its more local expression known as the North Sea Caspian pattern (NCP) (Barnston and Livezey 1987). The strengthening of the EA/WR in recent decades may have caused a reduction in winter precipitation in the Eastern Mediterranean although with little effect further east (Krichak and Alpert 2005). In late spring and early summer, the Indian Summer Monsoon (ISM) may also play an indirect role on precipitation in the southern Caucasus (Djamali et al. 2010; Rodwell and Hoskins 1996). In May, the interaction between the weakening low-pressure cells over the Black Sea and the westward displacement of ISM-related depressions over the Iranian plateau may determine which areas receive substantial May–June precipitation in this region (Djamali et al. 2010). The displacement of the Intertropical Convergence Zone (ITCZ) could have important implications for the precipitation regime in the region (Djamali et al. 2010).

Interactions of these superimposed atmospheric influences create complex climate patterns at different temporal scales. Because of the spatial and temporal complexity of climate, it is unlikely that instrumental meteorological records capture the full range of precipitation variability and the atmospheric dynamics that drive it. This issue is particularly acute across the Turkish Caucasus where these records are generally scarce or limited in time (Türkeş and Erlat 2003; Türkeş 1996). In other parts of the region, such as Georgia, Armenia or the lower elevations of the Greater Caucasus, these records are more abundant and some extend back to the 1890s. However, few records precede 1920 and many end around the 1990s (Menne et al. 2012; Vose et al. 1992). In this context, centennial-length records of precipitation are needed to determine past climatic variability, to place recent hydroclimatic conditions in a longer context, and resolve potential forcing factors. Tree-ring proxy data can help extend climate records past the instrumental period and broaden our knowledge on past precipitation variability.

There have been numerous climatic reconstructions in the eastern Mediterranean and central Turkey (Heinrich et al. 2013; Köse et al. 2011, 2013; Akkemik and Aras 2005; Akkemik et al. 2005, 2008; Touchan et al. 2003, 2005a, b, 2007; Griggs et al. 2007; Solomina et al. 2005). Most of these dendroclimatic reconstructions focused on

spring-summer precipitation, with May and June being the most common period and most of them used conifer species (e.g., *Cedrus libanii*, *Juniperus excelsa*, *Pinus nigra*). Until now the eastern most tree-ring based reconstruction in Turkey was developed for the central Anatolian highlands by D'Arrigo and Cullen (2001). A great limitation for dendroclimatic reconstructions in the Caucasus is a general lack of tree-ring chronologies from this region (but see Hughes et al. 2001; Touchan et al. 2014; Köse and Güner 2012).

Here, we use drought-sensitive tree-ring width chronologies from several species in Georgia and northeastern Turkey to estimate spring-summer rainfall in the Caucasus over the last two and a half centuries. Despite the high precipitation in the area, the presence of drought-sensitive old trees allowed us to recover a drought signal from tree-ring proxies. To overcome a potential dampening of the climate signal in tree rings, we use a multi-species approach as it has been shown to improve tree-ring based reconstructions of climate in temperate wet regions (Maxwell et al. 2011; Pederson et al. 2013; Cook and Pederson 2010). We used our reconstruction to characterize rainfall variability at interannual to multidecadal timescales and examine its associations with large-scale patterns of atmospheric circulation. Because no previous rainfall reconstructions exist for the Caucasus, we compared our reconstruction with independently derived precipitation reconstructions available for western Turkey.

2 Materials and methods

Our focus area for precipitation reconstruction was located in the western Caucasus. The region is dominated by steep-slope mountains with elevations ranging from 0 m asl on the Black Sea to over 5000 m asl in the Great Caucasus to the north. Because of the very high precipitation in the region, drought sensitive tree species are commonly restricted to sites such as the warm lower elevations in the Colchic floodplains and the south facing slopes of the mountains (Fritts 1976). We focused our sampling on this last type of locations where old trees were found. At five sites in the Lesser Caucasus of northeast Turkey (Fig. 1), we collected increment cores (1 or 2 cores per tree) from trees with external characteristics of old trees such as small crowns, twisted branches, and sinuous stems (Pederson 2010), of three conifers species and one broadleaf species (Table 1). *Abies nordmanniana* and *Picea orientalis* were sampled in two conifer-dominated forests at mid to high elevations (1600–1900 m asl) in inner valleys located leeward from the westerly prevailing winds. *Pinus pinea* trees growing in an area of relict Mediterranean vegetation within one of these valleys were cored at an elevation of 300–400 m asl. This is the easternmost *P. pinea* forest in the world and its origin, either relict or planted, is debated (Fallour et al. 1997). Regardless of origin, these trees dated back to at least 1773 CE. *Quercus petraea* were sampled in two sites on south-facing slopes between 600 and 900 m asl. Cores were air dried, mounted in grooved boards and sanded with progressive sand paper until the annual rings were clearly visible. The cores were later visually crossdated following standard dendrochronological procedure (Stokes and Smiley 1968). Tree-ring widths were measured with a 0.001 mm precision and crossdating was verified using the computer program COFECHA (Holmes 1983). In areas where chronologies were locally clustered and where we found a high degree of common agreement, collections were combined into one chronology. The *Quercus petraea* MUR chronology was created by pooling series from two sites located within 3 km of each other while the HAH and PAP chronology consisted of trees from two species of conifers, *A. nordmanniana* and *P. orientalis*.

In addition to these newly developed tree-ring width chronologies, we also used five chronologies developed from *Pinus sylvestris* trees from the area that were available at the International Tree-Ring Data Bank (ITRDB, available at: http://www.ncdc.noaa.gov/data-access/paleoclimatology-data/datasets/tree-ring). In this case, we selected chronologies with 20 or more ring width series and dating back to at least 1850.

Because there was evidence of exogenous disturbance in much of our collections, individual ring-width series were detrended using a spline function with a 50 % variance cutoff equal to two-thirds of the series length, using ARSTAN (Cook 1985). Prior to detrending the variance in individual series was stabilized using an adaptive power transformation (Cook and Peters 1997). We used the ARSTAN chronology, which retains the population-level autocorrelation and growth anomalies considered to be related to climate variability (Cook 1985). At the site level, individual ring-width series for each species were combined into annual chronologies using a biweight robust estimation of the mean. The quality of all the chronologies for dendroclimatic reconstruction was checked using the expressed population signal (EPS) statistic. For reconstruction purposes, the cutoff for each record was the first year of EPS >0.85, which is a threshold commonly used in dendroclimatology (Wigley et al. 1984).

We used gridded monthly precipitation data from the GPCC.v5 (Schneider et al. 2014) for the region between 38°–45°N and 38°–48°E. The GPCC data is well suited to represent precipitation patterns in areas with orographically induced precipitation surrounded by drier inland regions such as our focus region or the southern coast of the Caspian Sea (Schneider et al. 2014). For this area, we

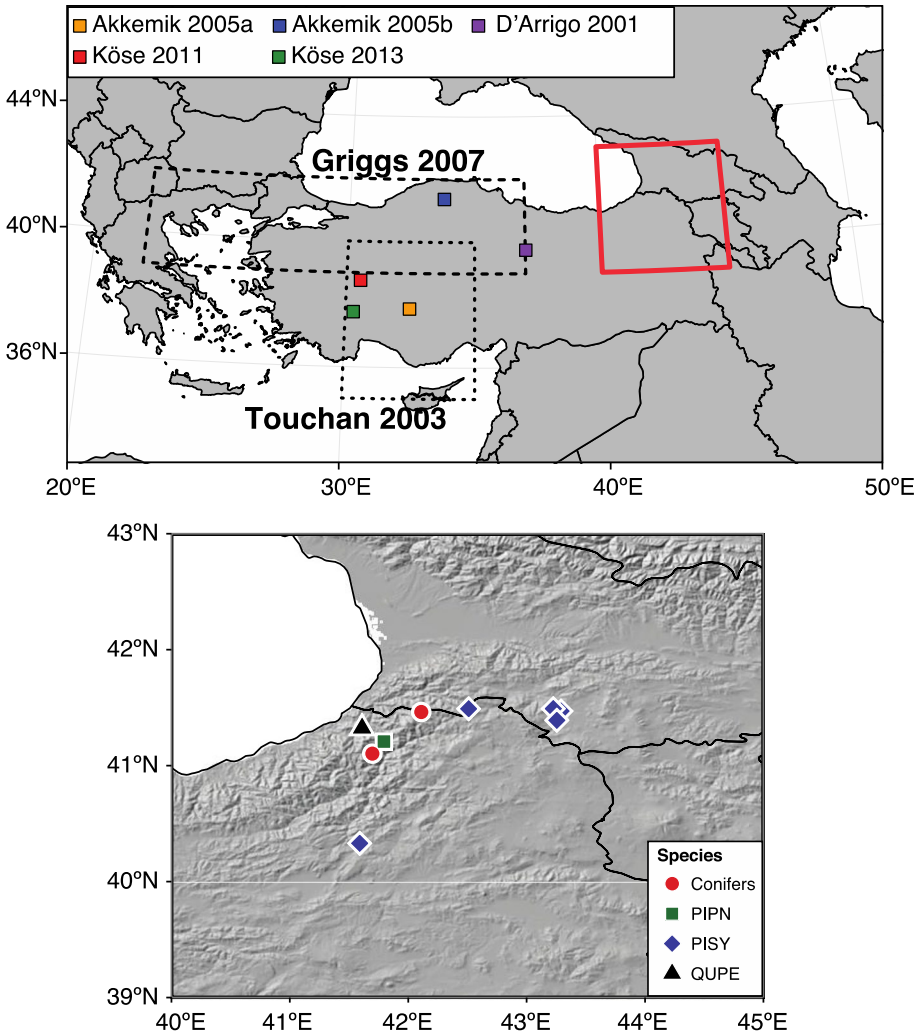

Fig. 1 Location of the study area. The *thick red box* represents the range of the gridded GPCC observed precipitation data used for reconstruction. The locations of previous precipitation reconstructions are also shown: Griggs et al. (2007), Köse et al. (2011, 2013), Akkemik et al. (2005), Touchan et al. (2003) and D'Arrigo and Cullen (2001). Lower map shows the locations and species of the tree-ring width site chronologies used as predictors. Species codes: PIPN, *Pinus pinea*; PISY, *Pinus sylsvestris*; QUPE, *Quercus petraea*; sites marked as "Conifers" include *A. nordmanniana* and *P. orientalis*

calculated the mean precipitation for periods of 1–6 months between previous June and current October. Climate sensitivity of all chronologies available from the area was evaluated against these seasonal regional precipitation means. Matching previous work (Touchan et al. 2014), our tree-ring network showed the strongest and most consistent significant correlations with precipitation during May and June. Because most of the precipitation records available for the area start around 1930, we restricted our calibration and verification periods to 1930–2001. Chronologies derived from the ITRDB limited the end of the calibration and verification period to 2001.

Because each chronology had different lengths, we used a nested reconstruction approach (Meko 1997) with principal component regression (PCR) (Cook et al. 1994) and split sample calibration and verification. With this nested approach, we were able to extend the length of the reconstruction beyond the common period of 1813–2001. Through this approach, we started with all selected chronologies during the common period and developed a PCR reconstruction. Then the shorter chronologies were dropped and a new PCR reconstruction was created. This way three 'backward nests' were created. Because the last year of the most recent chronology was 2013, just 12 years longer than the last year of the common period, we did not create any 'forward nests' (sensu Pederson et al. 2013).

In each nesting step, chronologies that correlated significantly (at $p < 0.1$) with May–June precipitation were considered. Principal component analysis (PCA) was performed on the correlation matrix of each nest's chronologies at year t and year t + 1, that is to account for the often-observed influence of previous year climate on current year tree growth (Fritts 1976). These resulting PCs were used as uncorrelated independent variables (predictors) to create a suite of regression models to estimate May–June precipitation. Model selection was performed by exhaustive search and the best-subset model was selected based on the calibrated Akaike's Information Criteria (AICc) and the Bayesian Information Criteria (BIC) for the complete period. No selection of the PC based on their explained variance was

performed previous to the PCR because components with small variance can also be important for the regression (Jolliffe 1982; Hill et al. 1977). These analyses were performed in R (R Development Core Team 2014) with the packages "vegan" (Oksanen et al. 2013) for PCA, and "leaps" (Lumley 2013) for exhaustive model search.

We conducted two split-sample calibration-verification tests to evaluate model performance and stability for each nest. The complete period (1930–2001) was divided into two equal-length periods, 1930–1966 and 1967–2001. For every nest, the transfer model was calibrated for the early (late) period and then validated with the late (early) period. Finally, the model was calibrated and validated for the complete period (1930–2001). The final reconstruction was developed with the model calibrated for the complete period. Three statistics, namely the adjusted coefficient of determination (R^2_{adj}), reduction of error (RE) and coefficient of efficiency (CE) were used to check the reconstruction skills of each nest (Cook et al. 1994). Positive values of RE and CE indicate predictive skill of the regression model, with CE generally being the most strict statistic to pass (Cook et al. 1994). This nesting procedure was reiterated until a nest accounted for less than 30 % of the May–June variation, or until RE or CE were negative for any test. If any of these criteria were matched, the model associated with that nest was considered insufficient for reconstruction and the nest not used. To account for potential changes in variance, each nest was normalized to the same mean and standard deviation of the most replicated nest. The final reconstruction was created by merging the older sections of each nest.

We analyzed the temporal variability of our reconstruction, in terms of oscillations and periodicity, by means of continuous wavelet transform (CWT) (Torrence and Compo 1998; Grinsted et al. 2004). Morlet wavelet function was used and the power was normalized by the variance to avoid bias with power at low periods. One of the advantages of the CWT is that no assumptions of stationarity are made and it can locate intermittent periodicities in a time frequency space. This analysis was performed in R (R Development Core Team 2014) with package "biwavelet" (Gouhier and Grinsted 2015).

The severity and duration of dry and wet periods were analyzed to characterize their persistence and cumulative deficit or surplus as deviations from the long-term mean. We estimated the return interval of these events as the time between two consecutive occurrences of events of similar duration. To assess how extreme these dry or wet events were within the entirety of the full reconstruction, we estimated the probability of observing an event of the same duration and intensity. For this, we calculated the thresholds for durations between 2 and 8 years, using 5000 randomized periods of the same duration drawing from the distribution of precipitation values in our time series and established significance at 5 % in a two-tail *t* test.

We analyzed our reconstruction in comparison with independent reconstructions of precipitation in the Middle East and Turkey available from previous studies based on tree-ring width chronologies (Akkemik and Aras 2005; Akkemik et al. 2005; D'Arrigo and Cullen 2001; Griggs et al. 2007; Köse et al. 2013; Touchan et al. 2003) (Fig. 1). Most of these studies also focused on spring-summer (May–June) precipitation.

The area is likely affected by different atmospheric circulation patters, mainly the NAO and EA/WR (Oguz et al. 2006) and the NCP (Kutiel and Türkeş 2005). We assessed the influence of these three patterns in our reconstruction. Because of the short period available for the EA/WR and the NCP indices (available at http://www.cpc.ncep.noaa.gov/data/teledoc/eawruss.shtml and http://www.cru.uea.ac.uk/cru/data/ncp/, respectively), only correlations were analyzed. The NCP is considered a local expression of the broader EA/WR. Thus we checked for intercorrelation between both indices during the seasons when they significantly correlated with observed or reconstructed precipitations. For NAO, however, we computed simple correlations and wavelet coherence (Torrence and Compo 1998; Grinsted et al. 2004) between different seasonal means of the index (Luterbacher et al. 2001, hereafter L01) and precipitation for the common period (1752–2001). In brief, the wavelet coherence (WTC) between the continuous wavelet transform of two time series allows to identify regions with high common power and locate them in the time–frequency space. The WTC analysis also provides information about the phase of that relationship, e.g., in phase, anti-phase or lags (see Grinsted et al. 2004 for a description of the method). The statistical significance of the WTC against red noise at the 10 % level was estimated using 1000 Monte Carlo randomizations. This analysis was performed in R (R Development Core Team 2014) and package "biwavelet" (Gouhier and Grinsted 2015).

It is of interest to explore the anomalous large-scale circulation conditions associated with unusual dry or wet spring-summer in the region during the instrumental period. For this purpose, we used a series of monthly gridded observational/reanalysis products, such as precipitation from GPCC version 6 (Schneider et al. 2014), winds and specific humidity from the twentieth century Reanalysis (Compo et al. 2011), sea level pressure (SLP) from the HadSLP2r product (Allan and Ansell 2006) and sea surface temperature (SST) from HadISST (Rayner et al. 2002). We defined years exhibiting extreme hydroclimatic conditions as those in the lowest and highest deciles of the observed and reconstructed May–June precipitation for the period 1930–2001. The sensitivity of the results to the number of extreme years selected was also assessed: while the magnitude of the anomalies varied somewhat, the spatial anomaly

patterns remained robust irrespective of the exact number of extreme years and thus results are only shown for deciles (Fig. 8). A two-tailed *t* test was used to determine whether the composite mean of the extreme years was significantly different from the mean of all years at each grid point.

3 Results

3.1 Chronology statistics

Here we present four new tree-ring width chronologies for the lesser Caucasus in northeastern Turkey from *Q. petraea* (MUR), *P. pinea* (HAT), and two that combine samples from *A. nordmanniana* and *P. orientalis* at two different sites (PAP and HAH) (Fig. 1; Table 1). The length of the nine tree-ring width chronologies that entered the more replicated nest ranged between 510 years (1498–2007) for the PAP site, composed of *A. nordmanniana* and *P. orientalis* trees, to 194 years (1813–2006) of the GEOR010 site of *P. sylvestris* (Table 1). TUR022 ended in 2001 and set the last year of our reconstruction. The period for which chronologies could be considered reliable for dendroclimatic reconstructions, EPS >0.85 (Wigley et al. 1984), started between 1540 CE and 1850 CE (Table 1). The relatively large difference between the absolute first year of some chronologies and their period of reliability was caused by low sample replication in the earlier period (e.g., TURK022 or MUR).

3.2 Regional climate

Because of the strong climate gradient in the western part of the Caucasus region, precipitation of individual gridded cells used in the reconstruction showed two distinct patterns (Appendix S1). Areas located to the west and close to the Black Sea coast had higher mean annual precipitation (Fig S1A) with a minimum in May–June (Fig S2A), which represented around 10 % of the annual precipitation (Fig. S1B). In contrast, the more interior areas had lower annual precipitation (Fig S1A) and a maximum monthly precipitation in May–June (Fig S2B), which accounted for over one-third of annual precipitation (Fig S1B).

3.3 Reconstruction

The nine tree-ring width chronologies in the full nest (1850–2001) accounted for 51.2 % of the variance of May–June precipitation for the period 1930–2001 (Fig. 2; Table 2). The second nest (1800–2001) included six chronologies and accounted for 49.5 %. The third and last nest (1752–2001), with just three chronologies, explained the lowest variance at 40.16 %. All nests and the different calibration and verification periods had positive CE and RE showing satisfactory predictive skills for all models and nests. The earliest nest (1752–2001) had the lowest values of CE and RE for the early calibration (1930–1966) and late verification (1967–2001) (Table 2). A longer reconstruction was hindered because the EPS of the chronologies that entered the three nests used decreased below 0.85 for earlier dates, or because nests with chronologies that extended back before 1752 CE had unsatisfactory R^2_{adj}, CE or RE statistics.

Reconstructed and gridded May–June precipitation exhibited common variability patterns at the interannual and decadal scales (Figs. 2, 3). According to our reconstruction, the region experienced the largest multiannual

Table 1 Summary statistics for the chronologies used in this study

Code	Species	Time span	First year EPS >0.85	N. cores (trees)	Lat (°N)	Lon (°E)	Elevation (m asl)	Source*
GEOR004	PISY	1776–2006	1800	47 (24)	41.47	43.29	1450	ITRDB[a]
GEOR005	PISY	1773–2006	1805	59 (26)	41.48	43.27	1100	ITRDB[a]
GEOR008	PISY	1767–2006	1790	26 (14)	41.46	43.32	1850	ITRDB[a]
GEOR010	PISY	1813–2006	1850	58 (29)	41.49	42.51	2010	ITRDB[a]
TURK022	PISY	1717–2001	1810	28 (n.a.)	40.33	41.59	2100	ITRDB[b]
HAT	PIPN	1773–2011	1800	18 (15)	41.21	41.79	380	this study
HAH	ABNO and PIOR	1667–2013	1745	33 (31)	41.10	41.70	1600–1900	this study
MUR	QUPE	1651–2013	1752	71 (41)	41.33	41.61	700–950	this study
PAP	ABNO and PIOR	1498–2007	1540	44 (23)	41.46	42.11	1750	this study

EPS, expressed population signal. An EPS >0.85 is considered the threshold for chronology reliability (Wigley et al. 1984)

n.a.: the number of different trees used for this chronology is not available

Species codes: ABNO, *Abies nordmanniana*; PIOR, *Picea orientalis*; PIPN, *Pinus pinea*; PISY, *Pinus sylsvestris*; QUPE, *Quercus petraea*

* ITRDB, chronologies archived at the International Tree-Ring Data Bank (available at http://www.ncdc.noaa.gov/data-access/paleoclimatology-data/datasets/tree-ring) and developed by (a) Ü. Buentgen, A. Nievergelt, A. Verstege, and (b) P.I. Kuniholm and N. Riches. GEO identifies chronologies from Georgia, TURK from Turkey

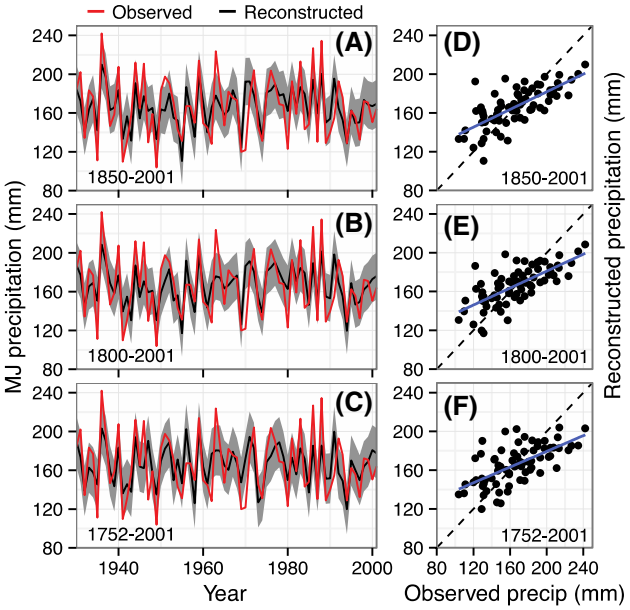

Fig. 2 Reconstructed (*black*) and observed (*red*) May–June total precipitation for the period 1930–2001 used for calibration and verification. *Left panels* show precipitation reconstructed with each of the three nests used **a** 1850–2001, **b** 1800–2001, and **c** 1752–2001. *Shaded area* represents RMSE. *Right panels* show scatter plots of reconstructed May–June precipitation for the different nested periods considered **d** 1850–2001, **e** 1800–2001, and **f** 1752–2001. *Dashed line* represents the 1:1 relationship for reference

changes of the twentieth century in the 1910s–1920s (Fig. 3a). The 1900s and mid 1910s had the driest May–June for multiannual periods, with 1909 and 1955 showing the lowest reconstructed precipitation of the century (below 2 SD; Table 3). The dry year 1909 was followed by a continuously wet period in the late 1910s and early 1920s. A similar, but smaller change in precipitation was again seen in the early 1930s (dry) and early 1940s (wet). Around the 1950s the region experienced a period of below average spring precipitation, although some years were close to normal. During this period, compared to instrumental precipitation, our reconstruction portrays dry years better than wet years. The wetter than average conditions from the 1960s until the late 1990s, however, were adequately represented by the tree-ring chronologies. The 1960–1990 extended wet period ended with an intense drought in the early 1990s that eased only around the year 2000 (Fig. 3a). A decrease in the precipitation variability from the beginning of the twentieth century onwards was evident (Fig. 3b).

Field correlations between our May–June precipitation reconstruction and the GPCC precipitation field for the period 1930–2001 revealed strong correlations across the entire target area (Fig. 4). These values were particularly strong (max r = 0.74, $p < 0.001$) around the area where most chronologies were located. Significant correlations were also observed outside the targeted area westward along the southern Black Sea coast, Central Anatolia and east to the Caspian Sea. These correlations decreased south towards Syria and Iraq and north of the Greater Caucasus. In western Russia north of the Sea of Azov, correlations were significant but negative.

Prior to the period of instrumental records, our reconstruction offers evidence of spring precipitation variability back to 1752. In our reconstruction, approximately 50 % of all drought events lasted just 1 year (droughts here being relative to the long-term mean of 166.9 mm, and 22.8 mm standard deviation). Droughts of 2 years accounted for 20 % of all drought events, with 17 % lasting for 3 years, and 13.5 % for 4 years or more (Fig. 5). The three strongest spring-summer droughts were reconstructed for 1851, 1955, and 1909 (Table 3). Periods of two consecutive years with precipitation below 1SD were reconstructed for 1764–1765, 1812–1813, 1833–1834, 1862–1863, and 1924–1925. The short but intense drought in 1851–1852 accumulated a deficit of 101 mm of precipitation, well above the 65.2 mm extreme threshold for events of that duration. The eight years between 1860 and 1867 was

Table 2 Results of the calibration and verification statistics between May–June precipitation and tree-ring width indices for the three nests reconstructed

Nest[a]	Calibration		Verification		Adj-R_c^2	RE	CE	Number of chronologies
1752	1930	1966	1967	2001	0.3499	0.3725	0.3661	3
	1967	2001	1930	1966	0.4277	0.4343	0.4298	
	1930	2001	1930	2001	0.4016	0.4039	n.a.	
1800	1930	1966	1967	2001	0.4421	0.4458	0.4401	6
	1967	2001	1930	1966	0.5633	0.5395	0.5358	
	1930	2001	1930	2001	0.4949	0.4961	n.a.	
1850	1930	1966	1967	2001	0.4331	0.4312	0.4254	9
	1967	2001	1930	1966	0.6061	0.5756	0.5722	
	1930	2001	1930	2001	0.5124	0.5107	n.a.	

[a] First year of the nest considered; Adj-R_c^2 adjusted coefficient of determination for the calibration period. RE, reduction of error; CE, coefficient of efficiency. n.a., not applicable

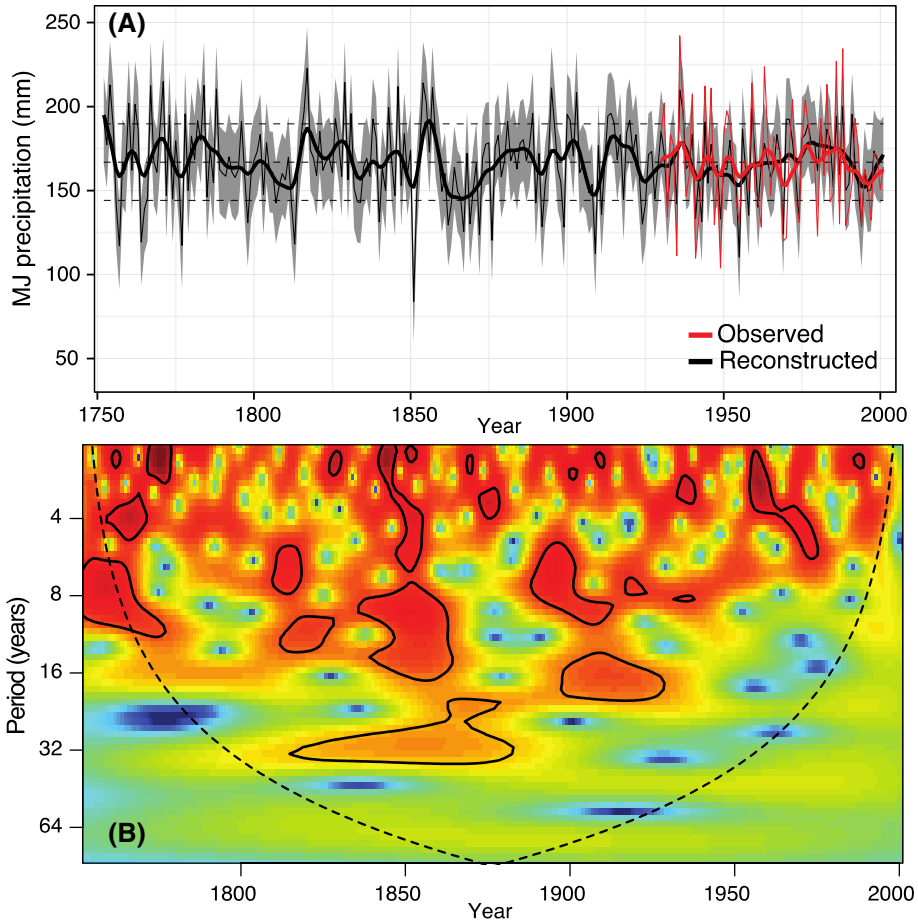

Fig. 3 Precipitation reconstruction for the Caucasus. Reconstructed (*black*) and observed (*red*) May–June total precipitation for the Caucasus. *Shaded area* represents RMSE for each of the three nests used. **b** Continuous wavelet power spectrum. *Black lines* show contours of 10 % significance level against red noise. The hatched line designates the cone of influence (COI) where edge effects might distort the results. Areas outside COI should not be interpreted

the longest period with below-average precipitation and accumulated a deficit of 169.3 mm (extreme threshold of 127.2 mm for 8 years). In contrast, three 6-year long droughts had reconstructed accumulated deficits between 68.3 and 100.5 mm, which are below the threshold for their occurrence to be considered extreme (116.6 mm for 6 years).

Considering positive precipitation anomalies, the wettest springs (2SD above long-term mean) of the entire period occurred between 1754 and 1854 (Table 3). Single years accounted for 50 % of all wet events; 2-year events were 25 % and 25 % lasted for 3 or more years. Multiyear wet periods ("pluvials") had estimated wet springs above 1SD during the nineteenth (1816–1817, 1854–1855) and the twentieth century (1913–1915, 1936–1937, and 1970–1971). The extreme 7-year pluvial, from 1853 to 1859, accumulated a rainfall surplus of 162 mm, but fell between two strong droughts (1851–1852 and 1860–1867).

Very dry and very wet years in our reconstruction showed good agreement with those described in previous

Table 3 Summary of dry and wet May–June from the reconstruction for the period 1752–2001

Precipitation	Years									
Very dry years (<2SD)	1757	1764	1777	1813	1851	1876	1909	1955		
Dry years (<1SD)	1756	1765	1798	1807	1812	1833	1834	1840	1862	1863
	1867	1869	1872	1890	1892	1899	1911	1924	1925	1932
	1935	1941	1943	1949	1958	1961	1969	1974	1994	
Wet years (>1SD)	1752	1760	1762	1767	1773	1778	1782	1788	1796	1816
	1826	1831	1838	1843	1846	1855	1857	1881	1889	1895
	1900	1901	1903	1913	1914	1915	1920	1936	1937	1944
	1959	1970	1971	1986	1988	1991				
Very wet years (>2SD)	1754	1771	1784	1817	1829	1854				

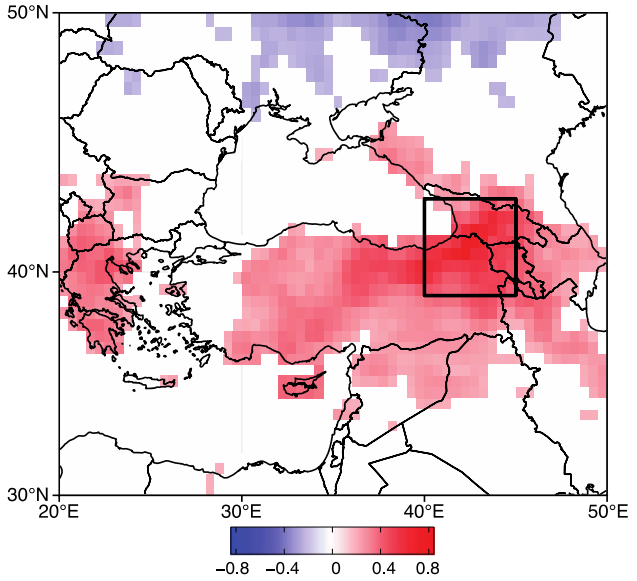

Fig. 4 Spatial correlation coefficients between reconstructed and observed (*red*) May–June precipitation for years 1930–2001. Only significant correlations ($p < 0.10$) are *colored*. The *black box* represents the range of the gridded GPCC gridded MJ precipitation data used for reconstruction

precipitation reconstructions for Turkey and the eastern Mediterranean (Table 4). All years with precipitation below 2 standard deviations from the reconstructed mean were also found dry or very dry (below 1SD) in two or more previous studies, except year 1876.

The analysis of the periodicities through continuous wavelet decomposition showed a diversity of frequencies between 4 and 30 years, with the more common being between 4 and 8 years. During the nineteenth and early twentieth century, longer frequencies (8–30 years) dominated the spectrum, whereas in the later part of twentieth century only shorter frequencies were significant (Fig. 3b).

Simple correlation analysis between seasonal means of NAO and instrumental gridded or reconstructed precipitation showed non-significant coefficients ($p < 0.05$). In the low-frequency domain, however, we found important and opposite variability between the reconstruction and previous JFM NAO (Fig. 6a). A comparison of both smooth time series showed that the most important drought (wet) periods in the record coincide with some of the most positive (negative) phases of the winter NAO (Fig. 6a). The WTC analyses also showed significant (10 % level) and inverse coherent powers at periods of 4, 8, and 16 years located between 1800 and 1950 (Fig. 6b). Both analyses showed that the exception to this patterns occurred in the droughts in 1810s and 1950s.

Our observed and reconstructed precipitation variability also showed links to two large-scale circulation patterns: the East Atlantic/Western Russia pattern (EA/WR) and the North Sea Caspian Pattern (NCP). The April–May

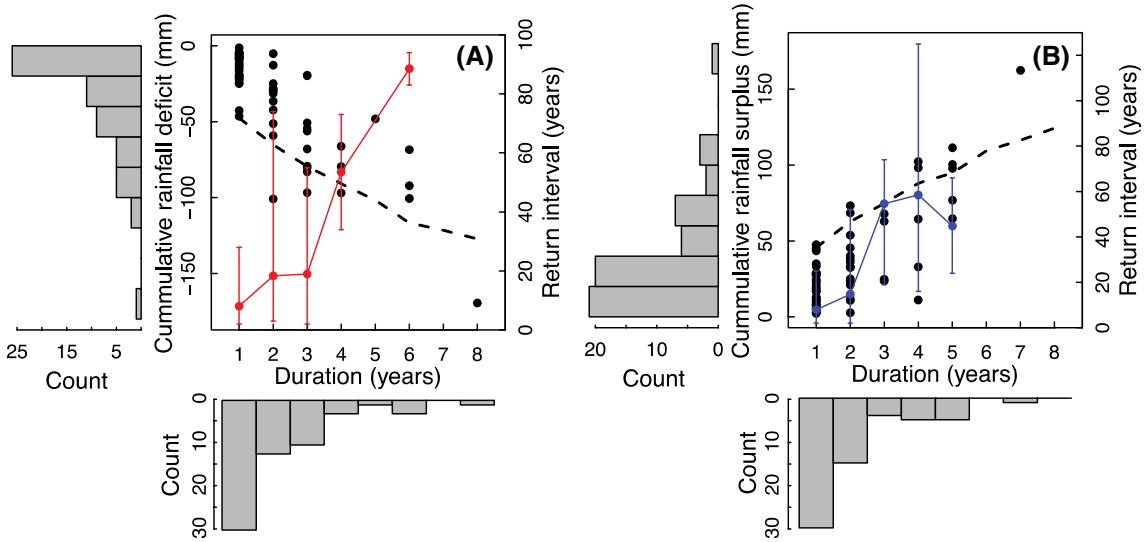

Fig. 5 Analysis of the severity and duration of **a** dry and **b** wet periods in the reconstructed May–June precipitation 1752–2001 (e.g. González and Valdés 2003). Dry (wet) years are identified as those years with reconstructed rainfall below (above) the reconstructed long-term mean. Duration is calculated for each dry (wet) event as the number of consecutive years with values below (above) the reconstructed long-term mean. Severity is estimated as the cumulative sum of the rainfall deficit (surplus) over those years. Events below (above) the *dashed line* are considered extreme ($p = 0.05$, two tail test) for a given duration and deficit (surplus). *Marginal histograms* indicate the frequency of droughts or wet periods of a given severity and duration. Return intervals for events were estimated as the mean time (in years) between the end and beginning of two consecutive events (dry or wet) with a given duration. The range (maximum and minimum) time between dry (wet) periods of a given duration are shown as *bars*

Table 4 Years with May–June classified as very wet or very dry (absolute departure >2SD) for the period 1752–2001, and comparison with previous work in Anatolia and the Eastern Mediterranean

Year	References
Very wet years (>2SD)	
1754	Touchan et al. (2003), Köse et al. (2013)
1771	Touchan et al. (2003), Akkemik et al. (2005), Akkemik and Aras (2005), D'Arrigo and Cullen (2001)
1784	Akkemik and Aras (2005), Köse et al. (2013)
1817	Griggs et al. (2007)
1829	Akkemik et al. (2005), Griggs et al. (2007), Köse et al. (2011)
1854	Akkemik et al. (2005), Griggs et al. (2007)
Very dry years (<2SD)	
1757	Akkemik et al. (2005), Akkemik and Aras (2005), D'Arrigo and Cullen (2001), Griggs et al. (2007)
1764	Touchan et al. (2003), Akkemik and Aras (2005), D'Arrigo and Cullen (2001), Griggs et al. (2007), Köse et al. (2011, 2013)
1777	Akkemik et al. (2005), Köse et al. (2011, 2013)
1813	Touchan et al. (2003), D'Arrigo and Cullen (2001)
1851	D'Arrigo and Cullen (2001), Griggs et al. (2007), Köse et al. (2011, 2013)
1876	
1909	Touchan et al. (2003), D'Arrigo and Cullen (2001), Köse et al. (2011, 2013)
1955	Akkemik et al. (2005), D'Arrigo and Cullen (2001), Griggs et al. (2007), Köse et al. (2011)

References were added if the reconstruction developed in the cited work showed at least a departure of 1SD in the same direction

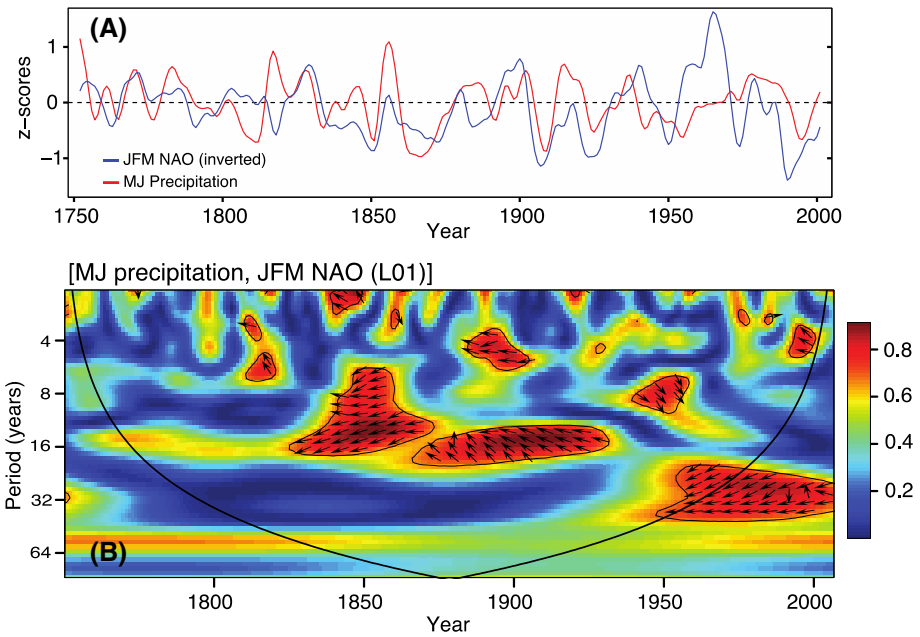

Fig. 6 Decadal variability of the reconstructed May–June precipitation (*red*) and the North Atlantic Oscillation index for January, February and March (JFM NAO, inverted axis; Luterbacher et al. 1999) between 1752–2001. The precipitation record has been converted to z-score for ease of comparison. *Lines* are a 10-year spline of the each annual record. **b** Squared wavelet coherence between MJ precipitation and JFM NAO index. In this case, original records (i.e., not smoothed) were used. *Black lines* show contours of areas 10 % significance level against red noise. The *hatched line* designates the cone of influence (COI); in areas outside of the COI, edge effects might distort the results and should not be interpreted. *Arrows* pointing to the *right* (*left*) show phase (anti-phase) behavior between the two time series

EA/WR atmospheric pattern was negatively correlated with May–June observed (r = −0.30, $p = 0.030$, $df = 50$) and reconstructed (r = −0.32, $p = 0.023$, $df = 50$) precipitation (Fig. 7). Positive and significant correlations were found between May–June NCP and observed (r = 0.34, $p = 0.014$, $df = 50$) and reconstructed (r = 0.34, $p = 0.013$, $df = 50$) May–June precipitation (Fig. 7). The length of the EA/WR and NCP (1950–2014) did not allow analyzing its decadal variability. It is important to note that the correlation between April–May EA/WR and May–June NCP was not significant (r = −0.04, $p = 0.772$, $df = 50$). Years with both a positive April–May EA/WR and a negative May–June NCP pattern (N = 16) were characterized by below average observed and reconstructed May–June precipitation (Fig S3).

Precipitation anomalies in the region during observed dry years showed that dry conditions (in excess of −25 mm/month) extend over much of the Caucasus towards the Caspian Sea and for much of Turkey and into Greece, while anomalous wet conditions occurred to the north of the Black Sea (Fig. 8a). The precipitation anomaly pattern is reversed for wet years (Fig. 8b). Extreme years based on our May–June reconstructions showed anomaly patterns in precipitation broadly consistent with those during observed years, though significant precipitation anomalies are more localized for the study region (Fig. 8a–d).

4 Discussion

4.1 Chronology development

In the western Caucasus, where annual precipitation can exceed 2500 mm and is well distributed throughout the year, drought sensitive tree species are commonly restricted to warm sites in the low elevations, south facing slopes with low soil development or the drier inner valleys (Fritts 1976). For this study, we have developed four new tree-ring width chronologies from the lesser Caucasus in north-eastern Turkey from a broadleaf species (*Q. petraea*) and three conifers (*P. pinea*, *A. nordmanniana*, and *P. orientalis*). These new sites constitute the most drought sensitive tree-ring width chronologies for the area to date. All five species used (including *Pinus sylvestris*) were important in developing a precipitation reconstruction for the spring and early summer. Particularly, oaks proved to be a key species in our precipitation reconstruction, which is in line with previous studies (Akkemik et al. 2005; Griggs et al. 2007). The oldest nest back to 1752 CE ends when the EPS of the MUR oak chronology falls below the commonly used threshold of 0.85. Using only chronologies with EPS >0.85 before that year did not allow to satisfactorily reconstruct precipitation.

The high precipitation in some parts of the Caucasus allows the development of luxurious temperate rainforest

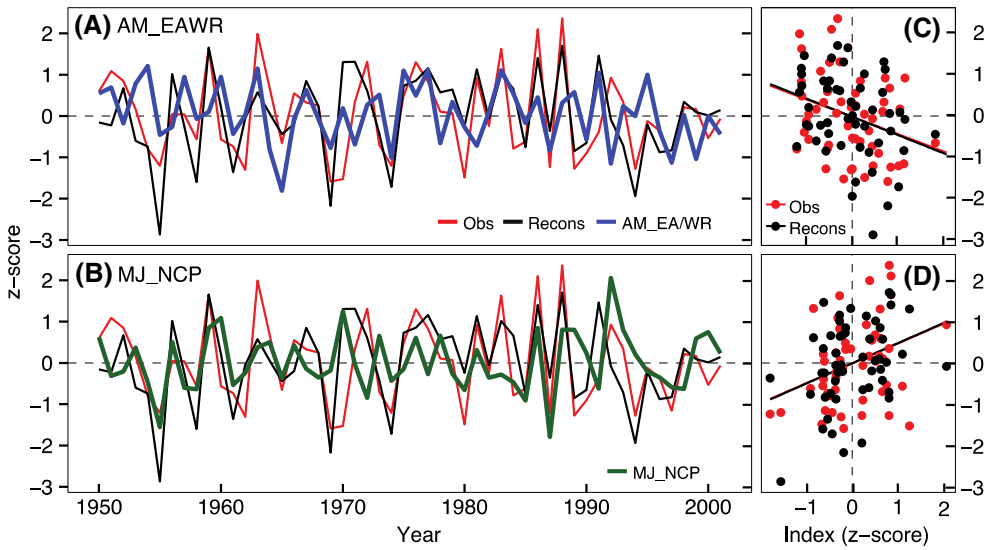

Fig. 7 Inter-annual variability of the reconstructed (*black*) and instrumental (*red*) May–June precipitation and **a** April–May East Atlantic/Western Russia teleconnection index (EA/WR, inverted) and **b** May–June North Sea Caspian pattern (NCP). Scatter plot of reconstructed (*black*) and instrumental (*red*) May–June precipitation against **c** EA/WR (r = −0.30 and $p = 0.0304$ for the reconstruction; r = −0.30 and $p = 0.0304$ for the observations) and **d** NCP index (r = 0.34 and $p = 0.013$ for the reconstruction; r = 0.34 and $p = 0.014$ for the observations). Both EA/WR and NCP index were standardized by the 1981–2010 climatology. Regression lines for reconstructed and instrumental precipitation were virtually indistinguishable for EA/WR and NCP. *Dashed line* represents the −1:1 relationship for reference

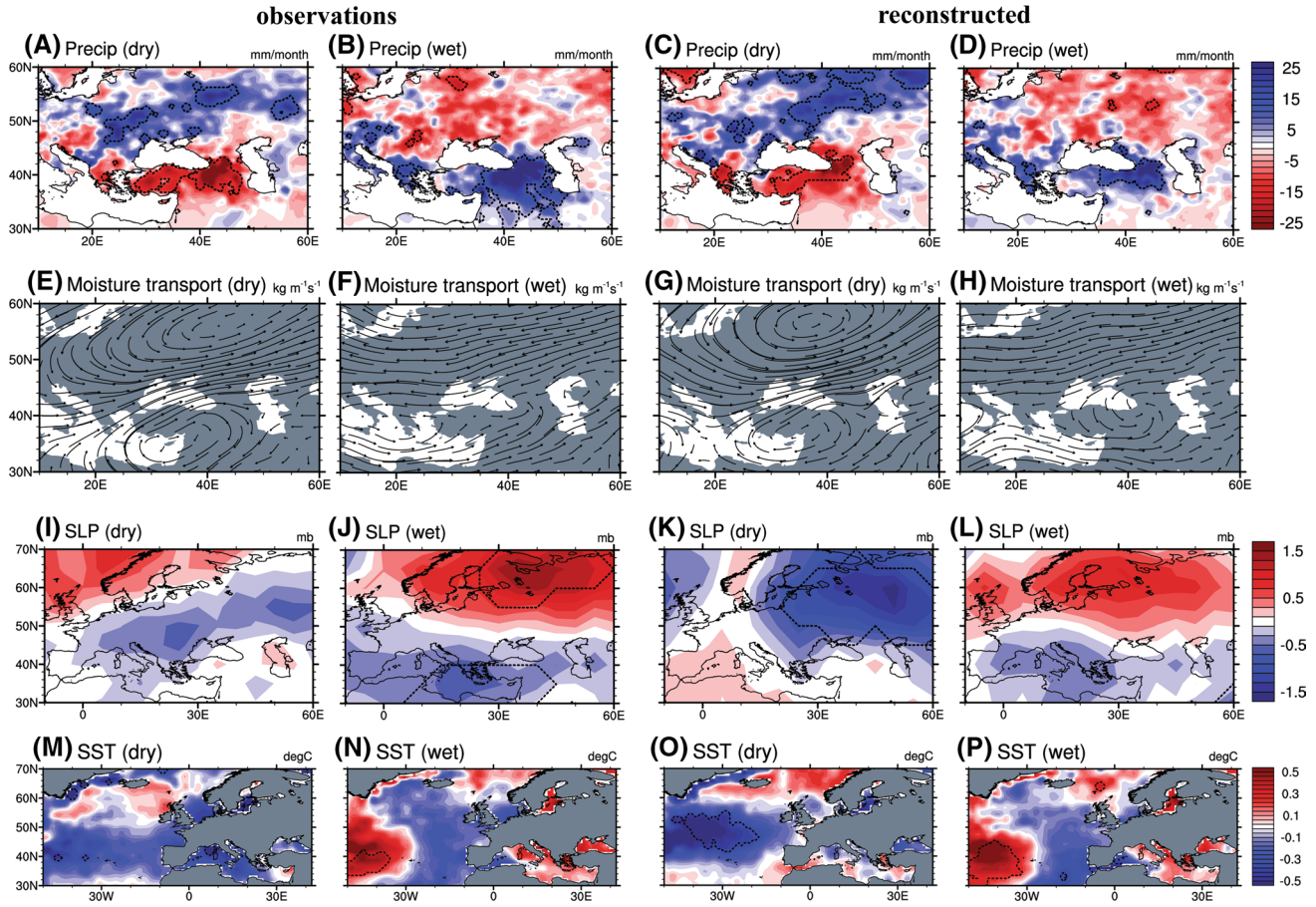

Fig. 8 Composite anomalies during extreme dry/wet years based on (*left*) observations and (*right*) reconstructed precipitation time-series for the study region for **a**–**d** precipitation (mm/month), **e**–**h** moisture transport (kg/m/s), **i**–**l** SLP (mb), and **m**–**p** SST (°C). *Dashed contours* delimit areas with anomalies significant at the 90 % confidence level in a two-tailed *t* test

vegetation but poses a potential challenge to reconstruct precipitation for the region because of the difficulty of finding sites of drought sensitive and long-lived trees. Most of our chronologies originate from forest with a certain degree of closed canopy conditions, and thus may have been affected by forest stand dynamics, unlike more classical drought sensitive open forest sites. In closed canopies forests, the effects of stand dynamics could obscure the climate signal at low frequencies recorded by tree-ring width. The strong agreement with reconstructions from other distant sites and species supports the feasibility of using less classical dendrochronological samples for climate reconstructions (Pederson et al. 2012) which helps overcome common problems in drought reconstructions from humid temperate forests (Cook et al. 1982). Including a diverse pool of species in our reconstruction likely reduces the probability that stand dynamics at any given site could have a great influence in the final reconstruction (Maxwell et al. 2011; Pederson et al. 2013; Cook and Pederson 2010). Our reconstruction will likely be improved by expanding the sampled area, extending chronology length from new drought-sensitive sites, and sampling new genera.

4.2 Reconstruction

Here we present the first tree-ring based reconstruction of spring-summer (May–June) precipitation variability for the Caucasus. This reconstruction demonstrates interannual and decadal climate variability back to 1752 CE, and shows that this variability was larger before the period of instrumental records. The positive calibration and verification performance of the three nests used in our reconstruction supports the use of tree-ring width chronologies from multiple tree species as proxies for past precipitation variability in this wet Caucasus region. This reconstruction provides an essential baseline that can be used to improve water resource management or evaluate the climatic effects on past vegetation changes, and could ultimately aid to improve forest management to adapt to new climate conditions.

We have reconstructed May–June precipitation which is the most commonly reported climate signal in dendroclimatic reconstructions from Anatolia and the eastern Mediterranean (Hughes et al. 2001; Touchan et al. 2003, 2014). Within our focus region, May and June are the driest months for the mesic areas (mainly in the west, close to the Black sea) and the wettest months in the drier areas to the east. Thus, May–June appears to be the period when precipitation is more critical for tree growth because it either represents the major water supply (semi-arid areas) or the time with the highest potential of water scarcity in mesic areas. The high common interannnual variability of May–June precipitation in the Caucasus was also supported by the strong field correlation between our reconstruction and the gridded precipitation North of the Greater Caucasus and west toward northern Anatolia. These correlations declined sharply towards the Caspian Sea and western Turkey (Fig. 4).

Based on our reconstruction, variability of spring precipitation was larger before the twentieth century, which confirms that the instrumental precipitation data is insufficient for adequately capturing the full range of rainfall variability. During the instrumental period (1930–2001), both the observed record and the reconstruction show two short periods of below-average May–June precipitation (early 1930s and late 1990s) and a longer, but less intense, spring drought around 1950. Tree rings recorded stronger droughts and pluvials prior to 1925. The largest swings between very dry and very wet conditions occurred between 1850 and 1870 (Fig. 3). Although most spring droughts lasted 3 years or less, longer periods of low May–June precipitation—up to 8 years—have occurred in the past (Fig. 5).

Previous tree-ring based reconstructions from the Middle East and Turkey show large precipitation variability over the last centuries. Despite the lower field correlations towards western Turkey, our reconstruction shows many similarities with other reconstructions from Turkey and the eastern Mediterranean hundreds of kilometers away (Fig. 9). For example, although D'Arrigo and Cullen (2001) reconstructed February-August precipitation for Sivas (central Anatolian highlands, ca 700 km west of our most western chronology), both reconstructions recorded several synchronous droughts (e.g. 1750s, 1850s, 1870s, 1910s) and pluvials (1900s, 1920s). The longest spring dry spell in the last 250 years in the Caucasus occurred in the 1860s and the 1870s and was only interrupted by individual years of average precipitation. This drought was also apparent in previous moisture reconstructions, though mainly in the northern half of eastern Anatolia (Akkemik and Aras 2005; Akkemik et al. 2005; Griggs et al. 2007; D'Arrigo and Cullen 2001; Köse et al. 2013). The strong drought of 1876 shown in our reconstruction was reported for various regions of Anatolia (Erinç 1949), but previous reconstructions in other parts of the Middle East and Turkey identified that year as wet or very wet (Köse et al. 2013; Akkemik and Aras 2005; Akkemik et al. 2005). Weaker, but widespread droughts found in most records during the pre-instrumental period also occurred in the 1750s, 1770s and 1850s. The single driest spring in our reconstruction was 1851, which was followed by a dry 1852. These 2 years were also two of the driest in studies as far west as the Aegean Sea and southwester Turkey (D'Arrigo and Cullen 2001; Griggs et al. 2007; Köse et al. 2013). Thus, we now find that the 1851–1852 drought was likely extensive across all Anatolia and the eastern Mediterranean.

There were also many similarities between the different reconstructions regarding wet periods. A short, but very wet period between two droughts in the early 1850s was

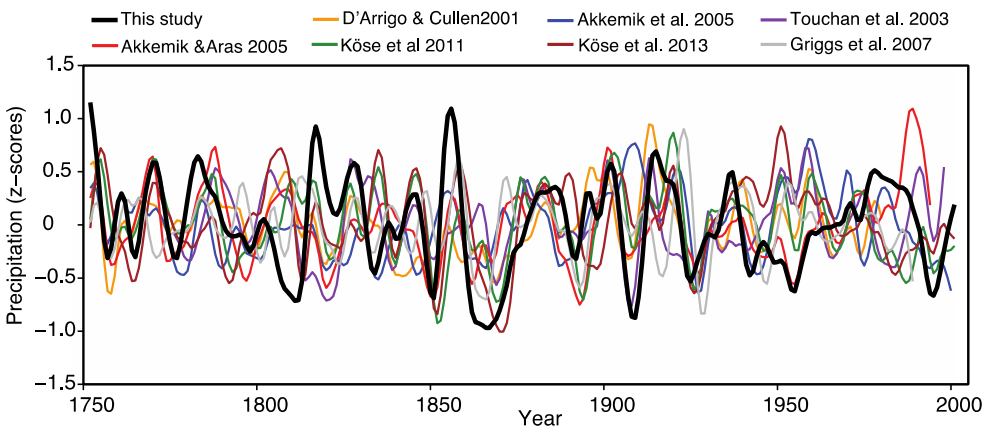

Fig. 9 Low-frequency variability of precipitation records across the eastern Mediterranean and Turkey reconstructed from tree-ring widths. Each *curve* is a 10-year spline of the each annual record. For ease of comparison, z-scores are used. Data sources for previous precipitation reconstructions: Akkemik and Aras (2005), Akkemik et al. (2005), D'Arrigo and Cullen (2001), Griggs et al. (2007), Köse et al. (2011, 2013), Touchan et al. (2003)

found in our reconstruction and previous studies (Akkemik and Aras 2005; Akkemik et al. 2005; Griggs et al. 2007; D'Arrigo and Cullen 2001). During the first half of the twentieth century, another sequence of wet and dry periods in our reconstruction was also observed simultaneously in previous reconstructions from northern Anatolia (Akkemik et al. 2005; D'Arrigo and Cullen 2001; Griggs et al. 2007). A denser tree-ring network would be desirable to resolve precipitation at finer spatiotemporal scales.

Interestingly, despite important similarities in precipitation variability during the first half of the twentieth century between all these reconstructions, they depict different trends after ca 1950. For example, south central Turkey showed a robust decline in precipitation from 1950, that eased at the end of 1990s (Akkemik and Aras 2005; Köse et al. 2013; Touchan et al. 2003), except for the reconstruction by Akkemik and Aras (2005) which showed wet conditions. In contrast, in the regions surrounding the Black Sea, both in northern Turkey (Akkemik et al. 2005) and in our reconstruction for the Caucasus, precipitation increased since 1950 until the mid 1990s or 1980s, respectively. These drying trends in the Mediterranean part of Turkey and positive around the Black Sea are in accordance with previous observations (Hoerling et al. 2012) and are projected to continue in the future (Evans 2009).

4.3 Climatology

Observed and reconstructed dry years over the study region were characterized by anomalous westerly moisture transport to the north of the Black Sea, while easterly moisture transport anomalies and more continental influences dominate over the study region, indicating a northward shift in the moisture transport accounting for the wet/dry dipole pattern to the north/south of the Black Sea (Fig. 8e). These changes in moisture transport are driven by negative sea level pressure (SLP) anomalies over central and southern Europe, extending eastward towards the Black Sea and into Russia, while positive SLP anomalies occur to the north over the British Isles and Scandinavia (Fig. 8i). The large-scale circulation and regional precipitation anomalies for the reconstructed dry years are very similar: they indicate strong anomalous westerly moisture transport to the north of the Black Sea into western Russia driven by the low pressure anomalies there, while anticyclonic conditions and easterly moisture transport anomalies characterize the Caucasus region and Turkey (Fig. 8g, k).

During the wet years, the circulation and pressure anomalies are reversed. A strengthened meridional pressure gradient and a southerly shift in the moisture transport and anomalous westerly flow occurs across the southern and eastern Mediterranean into Turkey and towards the Caucasus while easterly circulation anomalies dominate north of the Black Sea (Fig. 8f, j). The strongly decreased westerly circulation over central Europe could be associated with the negative phases of the NAO, which are also consistent with increased precipitation in the Mediterranean.

Our analyses also show relative coherence between low-frequency fluctuations in historical winter (January–February–March, JFM) NAO (Luterbacher et al. 1999) and spring-summer (May–June) precipitation over the Caucasus. Periods for which NAO and our reconstructed precipitation show greater disagreement coincide with those periods for which precipitation variability in the Caucasus differs from that of precipitation from parts of western Anatolia. Decadal winter NAO variability and reconstructed May–June precipitation in the Caucasus were closely coupled except for 1800–1830 and from 1950–1990 (Fig. 6). During these two periods, the variability of January–March NAO is larger than that of May–June precipitation and precipitation in the Caucasus exhibits negative deviations as compared to reconstructions from regions in the west (Fig. 9). These results suggest that the NAO is likely an important factor in the spatial coherence of low-frequency precipitation variability across Anatolia and the Caucasus, but also that the full range of long-term precipitation variability in our study area cannot be explained by NAO alone.

Previous studies show significant correlations between winter NAO and precipitation on the east Mediterranean mountains including the Caucasus and the mountains of Northeastern Turkey (López-Moreno et al. 2011). These correlations, however, were of opposite sign in the greater Caucasus in the north (positive) and the lesser Caucasus in the south (negative). All our tree-ring sites are located in the lesser Caucasus and reflect this negative correlation with winter NAO, although lagged. This lagged influenced of previous winter NAO on spring precipitation in the Caucasus and the eastern Mediterranean was hypothesized to be linked to variability patterns in Atlantic SST (Hercegbulić and Kucharski 2014). Our analyses also show that wet (dry) May–June conditions in the study region correspond to positive (negative) SST anomalies across the eastern Mediterranean and the Black Sea (Fig. 8n, p). Along with the westerly flow across these ocean regions, the unusually warm SST anomalies could contribute towards an enhanced moisture supply to the Caucasus. On longer time scales, Black Sea SST variability is associated with NAO forcing with a 2–3.5 year lag (Buongiorno Nardelli et al. 2010). Long-term SST changes may have also caused the observed changes in precipitation in the southern Black Sea coast during the Holocene (Göktürk et al. 2011; Kwiecien et al. 2009). A connection between rainfall in our study and NAO is also supported by the influence of this teleconnection pattern on tree-ring reconstructed February-August precipitation in central Anatolia (D'Arrigo and Cullen 2001) and on Tigris-Euphrates streamflow (Cullen and

deMenocal 2000). Cullen and deMenocal (2000) argued that the NAO affected rainfall in central Anatolia via modulating cyclogenesis in the Mediterranean and the Black Sea. The importance of cyclone track variability for precipitation in Turkey may be another consequence of the influence of Atlantic SST on regional climate (Karaca et al. 2000).

The high variability of May–June precipitation in the Caucasus is affected by the Siberian High retreating in the spring through the EA/WR (Ionita 2014) and the NCP (Kutiel and Kay 1992) and its interactions with the ISM (Vose et al. 1992) to further influence the precipitation pattern driven by common influence of cyclones (Karaca et al. 2000). The EA/WR and NCP atmospheric systems showed significant negative and positive correlations, respectively, with our reconstructed and observed precipitation for the period 1950–2001 at the interannual level. The superposition of a positive April–May EA/WR and a negative May–June NCP resulted in the most consistent drought patterns between 1950 and 2001. The positive effect of the negative phase of the EA/WR pattern on precipitation propagates southeast from mid-winter in western Europe to late spring towards the east (Ionita 2014). The location of the Caucasus also subjects the region to the remote forcing of the monsoon circulation (Djamali et al. 2010; Rodwell and Hoskins 1996). The pattern of SLP and wind anomalies for the dry years in our reconstruction agrees with the idea that a northwestward displacement of the monsoon effects towards Iran would result in a reduction of the spring precipitation over eastern Anatolia and the Caucasus (Djamali et al. 2010; Rodwell and Hoskins 1996). The effects of the EA/WR and NCP could be superimposed on the effect of the NAO to create a complex teleconnection pattern of climatic variability in the Caucasus, and broadly over the Black Sea (Krichak et al. 2002; Oguz et al. 2006; Ionita 2014). The SLP anomalies associated with extreme dry (wet) springs (Fig. 8i–l) are similar to those corresponding to the occurrence of positive (negative) NAO and EA/WR and negative (positive) NCP indices described by Krichak et al. (2002) and (Kutiel and Kay 1992). A denser network of sites expanding into the greater Caucasus could help discern a clearer pattern of atmospheric teleconnections in a region with complex geography between landmasses, medium sized sea basins (Black and Caspian seas) and strong altitudinal gradients.

Interestingly, the SST patterns during years with wet May–June conditions in our study region indicate anomalously warm SST conditions of +0.5 °C across the eastern Mediterranean and Black Sea (Fig. 8n, p). Recent Black Sea warming has amplified precipitation extremes causing flooding of catastrophic consequences (Meredith et al. 2015). Incidentally, the extreme wet hydroclimatic conditions leading to extensive flooding in Tblisi and Sotchi in early summer 2015 also coincided with anomalous warm SST anomalies of 2–4 °C across the eastern Mediterranean and Black Sea (not shown). The reverse conditions, with colder SST anomalies, though of weaker magnitude, can be seen during the dry years (Fig. 8m, o). Thus, further SST warming of the southeastern Black Sea (Buongiorno Nardelli et al. 2010) could lead to the intensification of extreme precipitations in the surrounding mountainous regions (Meredith et al. 2015)

5 Conclusion

We have developed the first precipitation reconstruction for the Caucasus using a network of ring width chronologies from six species. Based on our results, May–June precipitation before the period of instrumental records experienced larger interannual and decadal variability than during the last 70 years. Therefore, confirming that the instrumental records capture only a limited range of temporal scales of precipitation variability. The strongest droughts and pluvials for the last 250 years were recorded during the nineteenth century. Our results have also revealed important teleconnections between atmospheric circulation patterns and precipitation. While the NAO appears to affect precipitation variability at the low-frequency scale, EA/WR effects would be more apparent at the interannual timescales. In a region largely dependent on agriculture and where the occurrence of multiannual droughts (up to 8 year long as recorded by tree rings) could have potentially devastating effects, a better resolution of past precipitation variability is crucial to better understand the effects of each pattern (e.g. NAO, EA/WR) across different timescales. This could also contribute to better projections of precipitation trends at finer spatial scales and contribute towards improved management of water resources or evaluate effects of climatic changes on vegetation dynamics.

Acknowledgments The authors wish to thank Cengiz Cihan, Javier Martín Fernández, Mehmet Doğan, Marco Mina, Timothy Thrippleton and the Borçka-Artvin Forest Service for their generous assistance during fieldwork. We also thank Ü. Büntgen, A. Nievergelt, A. Verstege, N. Riches, and P.I. Kuniholm for making their tree-ring width chronologies available through the ITRDB. D. M-B was funded by Marie-Curie IEF Grant (EU-Grant 329935) and a Fulbright-Ministerio de Ciencia e Innovación (Spain) postdoctoral fellowships. This work was partially funded by Lamont-Doherty Earth Observatory, grants from the Climate Center of Lamont-Doherty Earth Observatory and from Istanbul University Research Fund (YADOP 33569). C. U. acknowledges support by NSF under AGS-1355339. LDEO contribution 7969.

References

Akkemik Ü, Aras A (2005) Reconstruction (1689–1994 AD) of April–August precipitation in the southern part of central Turkey. Int J Climatol 25(4):537–548

Akkemik U, Dagdeviren N, Aras A (2005) A preliminary reconstruction (A.D. 1635–2000) of spring precipitation using oak tree rings in the western Black Sea region of Turkey. Int J Biometeorol 49(5):297–302

Akkemik Ü, D'Arrigo R, Cherubini P, Köse N, Jacoby GC (2008) Tree-ring reconstructions of precipitation and streamflow for north-western Turkey. Int J Climatol 28(2):173–183

Allan R, Ansell T (2006) A new globally complete monthly historical gridded mean sea level pressure dataset (HadSLP2): 1850–2004. J Clim 19(22):5816–5842

Barnston AG, Livezey RE (1987) Classification, seasonality and persistence of low-frequency atmospheric circulation patterns. Mon Weather Rev 115(6):1083–1126

Chenoweth J, Hadjinicolaou P, Bruggeman A, Lelieveld J, Levin Z, Lange MA, Xoplaki E, Hadjikakou M (2011) Impact of climate change on the water resources of the eastern Mediterranean and Middle East region: modeled 21st century changes and implications. Water Resour Res 47:W06506. doi:10.1029/2010WR010269

Compo GP, Whitaker JS, Sardeshmukh PD, Matsui N, Allan RJ, Yin X, Gleason BE, Vose RS, Rutledge G, Bessemoulin P (2011) The twentieth century reanalysis project. Q J R Meteorol Soc 137(654):1–28

Connor SE, Thomas I, Kvavadze EV (2007) A 5600-yr history of changing vegetation, sea levels and human impacts from the Black Sea coast of Georgia. Holocene 17(1):25–36

Cook ER (1985) A time series analysis approach to tree-ring standardization. University of Arizona, Tucson

Cook ER, Pederson N (2010) Uncertainty, emergence, and statistics in dendrochronology. In: Hughes MK, Swetnam TW, Diaz HF (eds) Dendroclimatology: progress and prospects, developments in paleoecological research. Springer, Berlin

Cook ER, Peters K (1997) Calculating unbiased tree-ring indices for the study of climatic and environmental change. Holocene 7(3):361–370

Cook ER, Hughes MK, Kelly PM, Pilcher JR, LaMarche VC Jr (1982) Tree-ring data networks: comment. In: Hughes MK, Kelly PM, Pilcher JR, LaMarche VC Jr (eds) Climate from tree rings. Cambridge University Press, London, pp 6–7

Cook ER, Briffa KR, Jones PD (1994) Spatial regression methods in dendroclimatology: a review and comparison of two techniques. Int J Climatol 14(4):379–402

Cook BI, Smerdon JE, Seager R, Coats S (2014) Global warming and 21st century drying. Clim Dyn 43(9):2607–2627

Cullen HM, deMenocal PB (2000) North Atlantic influence on Tigris–Euphrates streamflow. Int J Climatol 20(8):853–863

D'Arrigo R, Cullen HM (2001) A 350-year (AD 1628–1980) reconstruction of Turkish precipitation. Dendrochronologia 19(2):169–177

Djamali M, Akhani H, Andrieu-Ponel V, Braconnot P, Brewer S, de Beaulieu JL, Fleitmann D, Fleury J, Gasse F, Guibal F, Jackson ST, Lezine AM, Medail F, Ponel P, Roberts N, Stevens L (2010) Indian summer monsoon variations could have affected the early-Holocene woodland expansion in the Near East. Holocene 20(5):813–820

Erinç S (1949) The climates of Turkey according to Thornthwaite's classifications. Ann Assoc Am Geogr 39(1):26–46

Evans JP (2009) Global warming impact on the dominant precipitation processes in the Middle East. Theor Appl Climatol 99(3–4):389–402

Fallour D, Fady B, Lefevre F (1997) Study on isozyme variation in *Pinus pinea* L.: evidence for low polymorphism. Silvae Genetica 46(4):201–206

Fritts HC (1976) Tree rings and climate. Academic Press, New York

Giorgi F, Lionello P (2008) Climate change projections for the Mediterranean region. In: International young scientists' global change conference 2003, vol 63, issue 2–3, pp 90–104

Göktürk OM, Fleitmann D, Badertscher S, Cheng H, Edwards RL, Leuenberger M, Fankhauser A, Tüysüz O, Kramers J (2011) Climate on the southern Black Sea coast during the Holocene: implications from the Sofular Cave record. Quat Sci Rev 30(19–20):2433–2445

Golubev YN, Kuftarkov AY, Golubeva ZA (1993) Seasonal fields of tangenital wind stress over the Black Sea. Phys Oceanogr 4(4):323–330

Gouhier TC, Grinsted A (2015) Biwavelet: conduct Univariate and Bivariate Wavelet Analyses. (version 0.17.5). http://github.com/tgouhier/biwavelet

Griggs C, DeGaetano A, Kuniholm P, Newton M (2007) A regional high-frequency reconstruction of May–June precipitation in the north Aegean from oak tree rings, A.D. 1089–1989. Int J Climatol 27(8):1075–1089

Grinsted A, Moore JC, Jevrejeva S (2004) Application of the cross wavelet transform and wavelet coherence to geophysical time series. Nonlinear Process Geophys 11(5/6):561–566

Heinrich I, Touchan R, Dorado Liñán I, Vos H, Helle G (2013) Winter-to-spring temperature dynamics in Turkey derived from tree rings since AD 1125. Clim Dyn 41(7–8):1685–1701

Herceg-Bulić I, Kucharski F (2014) North Atlantic SSTs as a Link between the Wintertime NAO and the following spring climate. J Clim 27(1):186–201

Hill RC, Fomby TB, Johnson SR (1977) Component selection norms for principal components regression. Commun Stat Theory Methods 6(4):309–334

Hoerling M, Eischeid J, Perlwitz J, Quan X, Zhang T, Pegion P (2012) On the increased frequency of Mediterranean drought. J Clim 25(6):2146–2161

Holmes RL (1983) Computer-assisted quality control in tree-ring dating and measurement. Tree-Ring Bull 43:69–78

Hughes MK, Kuniholm PI, Eischeid JK, Garfin G, Griggs CB, Latini C (2001) Aegean tree-ring signature years explained. Tree-ring Res 57(1):67–73

Ionita M (2014) The impact of the East Atlantic/Western Russia pattern on the hydroclimatology of Europe from mid-winter to late spring. Climate 2(4):296–309

Jolliffe IT (1982) A note on the use of principal components in regression. J R Stat Soc Ser C Appl Stat 31(3):300–303

Karaca M, Deniz A, Tayanç M (2000) Cyclone track variability over Turkey in association with regional climate. Int J Climatol 20(10):1225–1236

Kelley CP, Mohtadi S, Cane MA, Seager R, Kushnir Y (2015) Climate change in the Fertile Crescent and implications of the recent Syrian drought. Proc Natl Acad Sci 112(11):3241–3246

Köse N, Güner HT (2012) The effect of temperature and precipitation on the intra-annual radial growth of Fagus orientalis Lipsky in Artvin, Turkey. Turk J Agric For 36(4):501–509

Köse N, Akkemik Ü, Dalfes HN, Özeren MS (2011) Tree-ring reconstructions of May–June precipitation for western Anatolia. Quat Res 75(3):438–450

Köse N, Akkemik U, Guner HT, Dalfes HN, Grissino-Mayer HD, Ozeren MS, Kindap T (2013) An improved reconstruction of May–June precipitation using tree-ring data from western Turkey and its links to volcanic eruptions. Int J Biometeorol 57(5):691–701

Krichak SO, Alpert P (2005) Decadal trends in the east Atlantic–west Russia pattern and Mediterranean precipitation. Int J Climatol 25(2):183–192

Krichak SO, Kishcha P, Alpert P (2002) Decadal trends of main Eurasian oscillations and the Eastern Mediterranean precipitation. Theor Appl Climatol 72(3–4):209–220

Kutiel H, Kay PA (1992) Recent variations in 700 hPa geopotential heights in summer over Europe and the Middle East, and their influence on other meteorological factors. Theor Appl Climatol 46(2–3):99–108

Kutiel H, Türkeş M (2005) New evidence for the role of the North Sea—Caspian pattern on the temperature and precipitation regimes in continental central Turkey. Geogr Ann Ser A Phys Geogr 87(4):501–513

Kwiecien O, Arz HW, Lamy F, Plessen B, Bahr A, Haug GH (2009) North Atlantic control on precipitation pattern in the eastern Mediterranean/Black Sea region during the last glacial. Quat Res 71(3):375–384

López-Moreno JI, Vicente-Serrano SM, Morán-Tejeda E, Lorenzo-Lacruz J, Kenawy A, Beniston M (2011) Effects of the North Atlantic Oscillation (NAO) on combined temperature and precipitation winter modes in the Mediterranean mountains: observed relationships and projections for the 21st century. Glob Planet Change 77(1–2):62–76. doi:10.1016/j.gloplacha.2011.03.003

Lumley T (2013) Package 'LEAPS': regression subset selection. http://cran.r-project.org/web/packages/leaps/leaps.pdf

Luterbacher J, Schmutz C, Gyalistras D, Xoplaki E, Wanner H (1999) Reconstruction of monthly NAO and EU indices back to AD 1675. Geophys Res Lett 26(17):2745–2748

Luterbacher J, Xoplaki E, Dietrich D, Jones PD, Davies TD, Portis D, Gonzalez-Rouco JF, von Storch H, Gyalistras D, Casty C, Wanner H (2001) Extending North Atlantic oscillation reconstructions back to 1500. Atmos Sci Lett 2(1–4):114–124

Maxwell RS, Hessl AE, Cook ER, Pederson N (2011) A multispecies tree ring reconstruction of Potomac River streamflow (950–2001). Water Resour Res 47(5):W05512

Meko D (1997) Dendroclimatic reconstruction with time varying predictor subsets of tree indices. J Clim 10(4):687–696

Menne MJ, Durre I, Vose RS, Gleason BE, Houston TG (2012) An overview of the global historical climatology network-daily database. J Atmos Ocean Technol 29(7):897–910

Meredith EP, Semenov VA, Maraun D, Park W, Chernokulsky AV (2015) Crucial role of Black Sea warming in amplifying the 2012 Krymsk precipitation extreme. Nat Geosci 8(8):615–619

Nardelli BB, Colella S, Santoleri R, Guarracino M, Kholod A (2010) A re-analysis of Black Sea surface temperature. J Mar Syst 79(1–2):50–64

Oguz T, Dippner JW, Kaymaz Z (2006) Climatic regulation of the Black Sea hydro-meteorological and ecological properties at interannual-to-decadal time scales. J Mar Syst 60(3–4):235–254

Oksanen J, Blanchet FG, Kindt R, Legendre P, Minchin PR, O'Hara RB, Simpson GL, Solymos P, Stevens MHH, Wagner H (2013) Package 'vegan'. Community ecology package, version 2 (9)

Pavlova VN, Varcheva SE, Bokusheva R, Calanca P (2014) Modelling the effects of climate variability on spring wheat productivity in the steppe zone of Russia and Kazakhstan. Ecol Model 277:57–67

Pederson N (2010) External characteristics of old trees in the Eastern Deciduous Forest. Nat Areas J 30(4):396–407

Pederson N, Tackett K, McEwan RW, Clark S, Cooper A, Brosi G, Eaton R, Stockwell RD (2012) Long-term drought sensitivity of trees in second-growth forests in a humid region. Can J For Res 42:1837–1850

Pederson N, Andrew RB, Cook ER, Lall U, Devineni N, Seager R, Eggleston K, Vranes KP (2013) Is an Epic Pluvial Masking the Water Insecurity of the Greater New York City Region? J Clim 26:1339–1354

Rayner NA, Parker DE, Horton EB, Folland CK, Alexander LV, Rowell DP, Kent EC, Kaplan A (2002) Global analyses of SST sea ice and night marine air temperature since the late nineteenth century. J Geoghys Res 108:D14

Rodwell MJ, Hoskins BJ (1996) Monsoons and the dynamics of deserts. Q J R Meteorol Soc 122(534):1385–1404

Schneider U, Becker A, Finger P, Meyer-Christoffer A, Ziese M, Rudolf B (2014) GPCC's new land surface precipitation climatology based on quality-controlled in situ data and its role in quantifying the global water cycle. Theor Appl Climatol 115(1–2):15–40

Schubert SD, Wang H, Koster RD, Suarez MJ, Groisman PY (2014) Northern Eurasian heat waves and droughts. J Clim 27(9):3169–3207

Solomina O, Davi N, D'Arrigo R, Jacoby G (2005) Tree-ring reconstruction of Crimean drought and lake chronology correction. Geophys Res Lett 32:L19704. doi:10.1029/2005GL023335

Stanev EV, Rachev NH (1999) Numerical study on the planetary Rossby modes in the Black Sea. J Mar Syst 21(1–4):283–306

Stokes MA, Smiley TL (1968) An introduction to tree-ring dating. University of Chicago Press, Chicago

Tauger MB (2001) Natural disaster and human actions in the Soviet famine of 1931–1933. Carl Beck Pap Russ East Eur Stud 1506:67

R Development Core Team (2014) R: a language and environment for statistical computing. R Foundation for Statistical Computing, Vienna. http://www.R-project.org

Torrence C, Compo GP (1998) A practical guide to wavelet analysis. Bull Am Meteorol Soc 79(1):61–78

Touchan R, Garfin GM, Meko DM, Funkhouser G, Erkan N, Hughes MK, Wallin BS (2003) Preliminary reconstructions of spring precipitation in southwestern Turkey from tree-ring width. Int J Climatol 23(2):157–171

Touchan R, Funkhouser G, Hughes MK, Erkan N (2005a) Standardized precipitation index reconstructed from Turkish tree-ring widths. Clim Change 72(3):339–353

Touchan R, Xoplaki E, Funkhouser G, Luterbacher J, Hughes MK, Erkan N, Akkemik Ü, Stephan J (2005b) Reconstructions of spring/summer precipitation for the Eastern Mediterranean from tree-ring widths and its connection to large-scale atmospheric circulation. Clim Dyn 25(1):75–98

Touchan R, Akkemik Ü, Hughes MK, Erkan N (2007) May–June precipitation reconstruction of southwestern Anatolia, Turkey during the last 900 years from tree rings. Quat Res 68(2):196–202

Touchan R, Anchukaitis KJ, Shishov VV, Sivrikaya F, Attieh J, Ketmen M, Stephan J, Mitsopoulos I, Christou A, Meko DM (2014) Spatial patterns of eastern Mediterranean climate influence on tree growth. Holocene 24(4):381–392

Trigo RM, Gouveia CM, Barriopedro D (2010) The intense 2007–2009 drought in the Fertile Crescent: impacts and associated atmospheric circulation. Agric For Meteorol 150(9):1245–1257

Türkeş M (1996) Spatial and temporal analysis of annual rainfall variations in Turkey. Int J Climatol 16(9):1057–1076

Türkeş M, Erlat E (2003) Precipitation changes and variability in Turkey linked to the North Atlantic oscillation during the period 1930-2000. Int J Climatol 23(14):1771–1796

Vose RS, Schmoyer RL, Steurer PM, Peterson TC, Heim R, Karl TR, Eischeid J (1992) The Global Historical Climatology Network: long-term monthly temperature, precipitation, sea level pressure, and station pressure data, vol 3912. Oak Ridge National Laboratory, Oak Ridge

Wigley TML, Briffa KR, Jones PD (1984) On the average value of correlated time series, with applications in dendroclimatology and hydrometeorology. J Appl Meteorol 23(2):201–213

Xoplaki E, Gonzalez-Rouco JF, Luterbacher Ju, Wanner H (2004) Wet season Mediterranean precipitation variability: influence of large-scale dynamics and trends. Clim Dyn 23(1):63–78